

Lattice dynamics in second-stage bromine-graphite intercalation compound

Ch. Simon, F. Batallan, and I. Rošenman

*Groupe de Physique des Solides de l'Ecole Normale Supérieure,
Laboratoire associé au Centre National de la Recherche Scientifique, Tour 23,
2 Place Jussieu, 75251 Paris Cedex 05, France*

H. Lauter

Institut Laue-Langevin, 156X, 38042 Grenoble Cedex, France

G. Furdin

*Laboratoire de Chimie Minérale Appliquée (A. Herold),
Laboratoire associé au Centre National de la Recherche Scientifique,
Université de Nancy I, CO 140, 54037 Nancy Cedex, France*

(Received 6 May 1982)

We have studied by coherent inelastic neutron scattering the phonon spectrum of a second-stage bromine-graphite intercalation compound. The intercalate sample was obtained from highly oriented pyrolytic graphite. We have observed the almost complete low-energy (< 12 THz) phonon spectrum with longitudinal and transverse phonons propagating along the c direction as well as in the layer plane. We have observed three branches polarized along the c axis which present energy gaps along the c direction. The acoustic branch propagating in the layer plane contrary to the optic ones is very sensitive to the intercalate. The main character of the modes polarized in the layer plane is the dispersionless optic branch along the c direction at 1 THz. A phenomenological Born–von Kármán force-constant model with nonaxial symmetry, developed in order to interpret our results, explains them very well.

I. INTRODUCTION

Graphite intercalation compounds (GIC's) are, like graphite itself, layered materials. The great variety of molecules which can be intercalated as well as the possibility given by the existence of stages (i.e., the number of graphite layers between two adjacent intercalate layers) for a given intercalated species, allows us to prepare materials with a large variation of the anisotropy in their properties.^{1,2} For example, the ratio of the out-of-plane to the in-plane resistivity can be varied from 10 to 10^6 . This anisotropy is also observed in other electronic properties such as the Fermi surface. Therefore, it would be interesting to study how this anisotropy of the electronic properties is reflected in the lattice dynamics.

Many investigations on high-energy lattice modes near 47 THz (1600 cm^{-1}) have been made by using Raman effect^{2,3} and infrared absorption.^{2,4} These modes present a fine structure, but their values are very close to the corresponding ones of pristine graphite. These studies only give information about the Γ point of the Brillouin zone.

At lower energies some results obtained by inelastic neutron scattering on different GIC's have been published. The first studies^{5–7} were limited to the longitudinal modes propagating along the direction perpendicular to the layers (c axis). In KC_{36} Magerl and Zabel⁷ have observed energy gaps for these phonons and explained their results by using a rigid-layer model. In RbC_8 Kamitakahara *et al.*⁸ have observed phonons polarized in the c direction and propagating both along the c axis and in the basal plane.

Two theoretical calculations of the phonon dispersion relations using the Born–von Kármán force-constant model have been recently published.^{9,10} However, no extensive experimental investigation of the phonon spectrum of these compounds has yet been made.

We present here the first such study of the phonon dispersion relations in a GIC. We have chosen as intercalation compound the second stage C_{14}Br . We have observed phonons at low energies, less than 12 THz, polarized both perpendicular to and in the layer plane and propagating both perpendicular to and in the layer directions. A short report on this

work has been published elsewhere.¹¹ We interpret our results by using a Born–von Kármán force-constant model and adjust the phenomenological parameters in agreement with our results.

In Sec. II we present the experimental aspects related to both the sample and measuring technique. Section III is devoted to the experimental results. In Sec. IV we summarize the results on the lattice dynamics of pure graphite. In Sec. V we interpret our results and we elaborate a phenomenological Born–von Kármán force-constant model. Then in Sec. VI we discuss our results. The conclusion of this work is given in Sec. VII.

II. EXPERIMENTAL ASPECTS

We have chosen stage two of bromine GIC for this phonon study. This intercalate is a very simple molecule and there are several published works about its structural and electronic properties.^{12–14} Moreover the bromine atom is a good candidate for neutron studies [$\sigma_{\text{coh}}=5.81$ barn, $\sigma_{\text{inc}}=0.1$ barn, and $\sigma_{\text{abs}}=6.7$ barn (Ref. 15)].

The starting material is HOPG (highly oriented pyrolytic graphite). The intercalation is made by direct action of bromine gas on the HOPG held in a quartz container. After the intercalation, the container is sealed in the presence of excess bromine gas.

As there is some controversy about the composition of the bromine second-stage GIC (Refs. 12 and 13) we have undertaken a thermogravimetric and a structural study on the bromine GIC family. The richest bromine GIC is a stage-2 compound and corresponds to the chemical formula C_8Br . Its desorption gives stable compounds of chemical formulas C_{14}Br , C_{21}Br , and C_{28}Br of stages 2, 3, and 4, respectively. We have prepared a desorption compound to investigate the intralayer ordering of bromine by neutron diffraction. In the range of temperatures between 300 and 10 K the Bragg peaks do not change significantly. The corresponding unit cell is given in Fig. 1. These peaks correspond to the main Bragg peaks given by Eeles and Turnbull¹³ but these authors also observed some additional weak peaks which were indexed by them in a larger unit cell. Our cell is eight times smaller than this one. A complete report of this work will be published elsewhere.

The dimensions of the sample that we have used for inelastic scattering were $42 \times 15 \times 4$ mm³ after intercalation. We have made two runs of measurements with this sample. The stage was measured at the beginning of each run by (00 l) neutron diffraction. The sample was found to be nonhomogeneous. It is formed by zones of stages 2 and 3. In the first

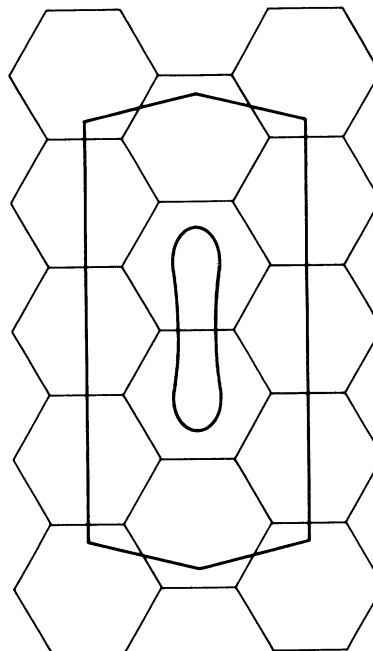


FIG. 1. Unit cell in the layer plane of the bromine GIC $\text{C}_{7.5}\text{Br}$ as obtained by neutron-diffraction studies. The hexagonal array represents the graphite lattice.

cycle of experiments the composition was about 75% of stage 2 and 25% of stage 3. For the second cycle, six months later it was about 33% of stage 2 and 66% of stage 3. These zones correspond to the chemical formulas C_{14}Br and C_{21}Br as tested by study of the ($hk0$) bromine circles by neutron diffraction.

The experiments were performed on the triple-axis neutron spectrometer IN8 at the high-flux neutron reactor of the Institute Laue-Langevin in Grenoble. At low energies, less than 6 THz, the (002) planes of HOPG were used as the monochromator, but at high energies, we have used the (111) planes of copper. The analyzer always used the (002) planes of HOPG. When necessary we have used a HOPG filter to eliminate the harmonic frequencies.

We have made experiments at 300 and 10 K. There are only small differences between the results. Here we will only describe the results for 300 K. The experimental scans are fitted by a sum of Gaussian peaks with a linear background, except for the case described in Fig. 5.

III. EXPERIMENTAL RESULTS

The unit cell of single crystalline graphite contains two layers and four atoms. The basic vectors

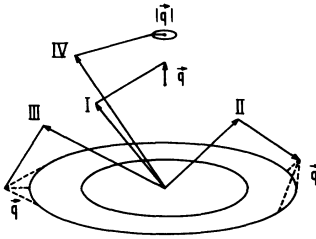


FIG. 2. Reciprocal space diagram for GIC obtained from HOPG showing the four experimental neutron scattering configurations used in this work.

are $a=b=2.45 \text{ \AA}$, $c=6.70 \text{ \AA}$, $\alpha=\beta=\pi/2$, and $\gamma=\pi/3$. The reciprocal lattice is given by $a^*=b^*=4\pi/a\sqrt{3}$ which defines the basal plane, $c^*=2\pi/c$, $\alpha=\beta=\pi/2$, and $\gamma=2\pi/3$. The reciprocal lattice of HOPG is that of single crystalline graphite with a random rotation about the c^* axis. The HOPG diffraction pattern is then made of concentric circles in the planes perpendicular to the c^* axis except on the c^* axis itself.

In the same way the diffraction pattern of the GIC obtained from HOPG is made of points along the c^* axis which correspond to the identity period I_c of the GIC, and families of concentric circles centered on the previous points and in a plane perpendicular to the c^* axis. These circles correspond to

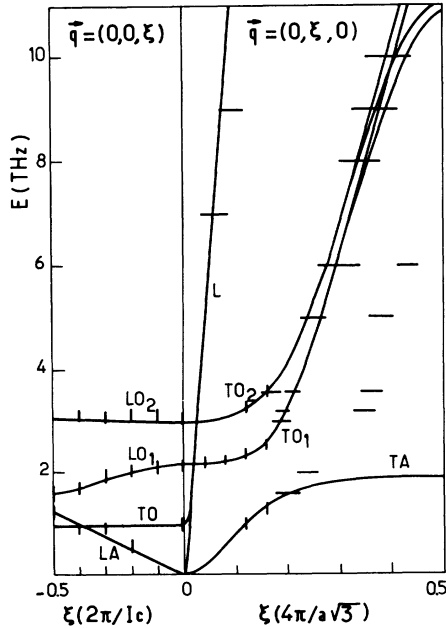


FIG. 3. Phonons observed in the stage-2 bromine GIC. The vertical and horizontal bars are the experimental errors of constant- Q and constant-energy scans, respectively. The continuous lines are the results of the Born-von Kármán force-constant model discussed in the text.

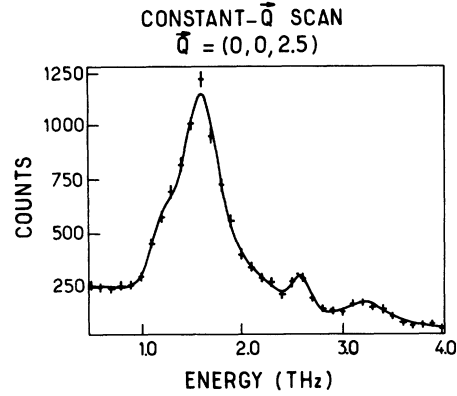


FIG. 4. Constant- Q scan for the $[001]L$ phonons at the zone boundary. The main peak is a doublet which corresponds to the gap. The peak observed at 3.3 THz corresponds to the second optic branch of stage 2. The peak at 2.6 THz belongs to stage 3.

those of HOPG or arise from the intercalate layer lattice.

We have used a scattering plane containing the c axis of the sample. This geometry allows us to study all the phonons in GIC's obtained from HOPG. We have represented the phonons in a reciprocal cell defined by the following three vectors: $\langle 100 \rangle$ and $\langle 010 \rangle$ are the basal vectors a^* and b^* of

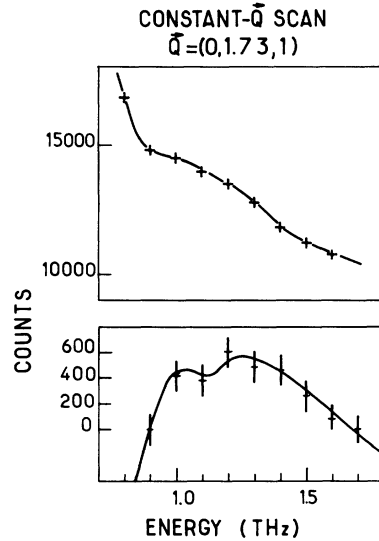


FIG. 5. Constant- Q scan for the $[001]T$ phonons at the Γ point. The upper figure presents the experimental value and the lower one the same results in which we have subtracted a Gaussian elastic peak. The vertical bars are the experimental errors. The full line represents the results of a fit by two asymmetric peaks similar to those calculated by Nicklow *et al.* The lower-energy one corresponds to the second-stage compound and the upper one to the third-stage one.

the reciprocal space of graphite defined above. The third vector $\langle 001 \rangle$ is along the c^* axis and is $2\pi/I_c$ long.

As our sample is a mixing of stages we have observed phonons belonging to zones of stage 2 and zones of stage 3. The identity period along the c axis is different for stages 2 and 3. The phonon branches then present a translation invariance which depends on the stage. That allows us to attribute a branch to a given stage for the $[001]$ phonons. In the layer plane, this difference does not exist and we have made the attribution by continuity at the Γ point with $[001]$ branches. As we are here interested mainly in the second-stage compound we have used the unit cell which corresponds to it ($I_c = 10.30 \text{ \AA}$).

We have used four different experimental configurations which are defined in Fig. 2. Figure 3 summarizes the experimental results for the phonon-dispersion relations attributed to stage two and which we shall describe now.

With the configuration I we study the $[001]L$ phonons propagating and polarized along the c axis. We have observed low-energy ($< 4 \text{ THz}$) branches that one can follow all over the Brillouin zone and on many Brillouin zones. This allows us to separate the phonons of stage 2 from those of stage 3. For stage 2 we have observed three branches which present energy gaps. Figure 4 shows this gap at the zone boundary. These results are very similar to those previously published⁷ on other GIC's.

Configuration II allows us to investigate the $[001]T$ phonons propagating along the c axis and polarized in the layer plane. These phonons are much more difficult to observe. They are located at very low energy ($\sim 1 \text{ THz}$) and are observed superimposed on the elastic peak. Moreover these phonons are degenerate: One observes many phonons at the same point of reciprocal space as shown in Fig. 2. We have observed them near the (111) point, which is in fact the $(0\sqrt{3}1)$ point of our scattering plane. In order to take into account both facts, we have fitted these scans with a Gaussian elastic peak added to the asymmetric peaks calculated by Nicklow *et al.*¹⁶ in pure graphite. Moreover, the peaks which correspond to both observed stages are mixed. Figure 5 shows an example of this situation. The branch that we have obtained in this configuration seems flat.

Configuration III was used to study phonons which are propagating and polarized in the layer plane. In particular this configuration gives the $[010]L$ phonons but also some transverse ones. These phonons are observed at higher energies in constant-energy scans. These peaks are very sharp, which means that these phonons are probably very isotropic and independent of stage. Figure 6 shows

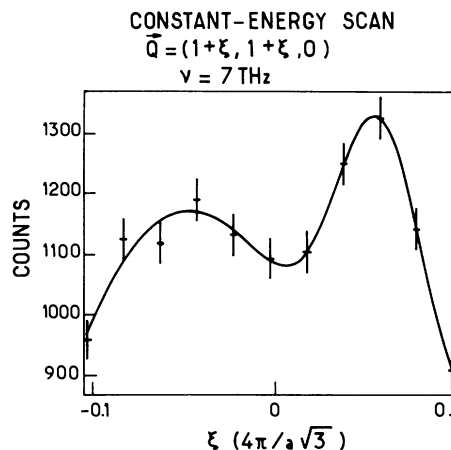


FIG 6. Typical constant-energy scan which shows the $[010]L$ phonons.

a typical scan in this configuration. The corresponding branch is linear.

Configuration IV allows us to study the $[010]T$ phonons which are propagating in the layer plane and polarized along the c axis. In this configuration we fix only the modulus of \vec{q} and observe all the directions of the layer plane in the same point. In this configuration the phonon spectrum is very rich.

For stage 2 we have observed three branches by constant- \vec{Q} scans for low \vec{q} (less than half of the length of the Brillouin zone) and low energy ($< 4 \text{ THz}$). The $[010]T$ optical branches are connected to the $[001]L$ optical branch at the Γ point and are almost degenerate at high energies where they are observed as single broad peaks. They reach the zone boundary at about 12 THz. In Figs. 7(a) and 7(b) we show this evolution. The acoustical branch is more difficult to observe and we do not know where it reaches the zone boundary. The behavior of this branch will be explained later in light of our model.

IV. THE LATTICE DYNAMICS OF GRAPHITE

We summarize here some results of the lattice dynamics of graphite because they present many common aspects with those of the GIC and we will use them in the interpretation of our results. As graphite has four atoms in its unit cell there are 12 vibrational normal modes at $\vec{q}=0$. Three of them are acoustical. In Table I we report the experimental data relative to the optical modes.¹⁶⁻¹⁹

The first study of lattice dynamics of graphite using inelastic neutron scattering was made by Dolling and Brockhouse.²⁰ Nicklow, Wakabayashi, and Smith¹⁶ used a HOPG sample. They have observed low-energy phonons ($< 14 \text{ THz}$) in the four experi-

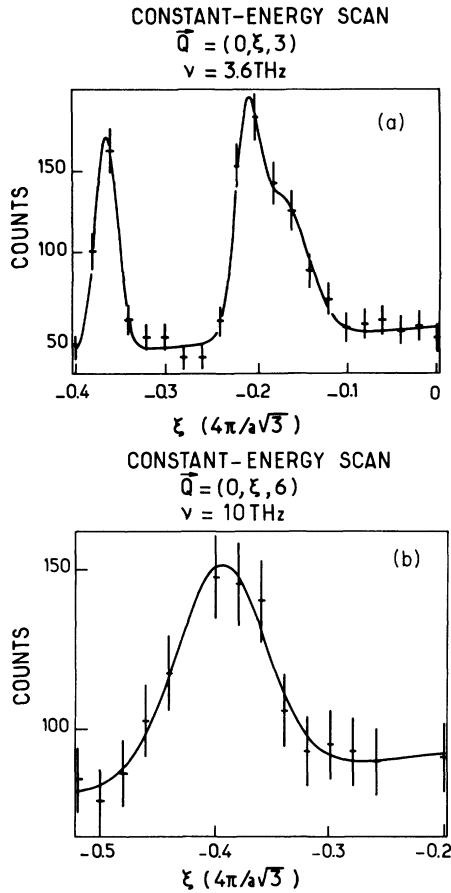


FIG. 7. Two constant-energy scans for the $[010]T$ phonons. (a) At 3.6 THz these phonons are well separated but (b) they are degenerated in a broad peak at 10 THz.

mental configurations shown in Fig. 2.

Their results are summarized in Fig. 6 of their article.¹⁶ For each of the phonons $[001]L$ and $[001]T$ they have observed at very low energy (<4 THz) two branches without any energy gap. For the $[010]L$ phonons they have observed a linear branch which joins the $[001]T$ branches at the Γ point. For the $[010]T$ phonon they have observed two branches which join the $[001]$ branches at the Γ point. These branches are almost parabolic at low energies (<6 THz) and linear from 6 to 14 THz where $|\vec{q}| = 2\pi/\sqrt{3}a$.

They have interpreted their results by using a simple axially symmetric Born–von Kármán force-constant model. They have adjusted the force constants to their experimental results and to the experimental value of the Raman-active mode $E_{2g}^{(2)}$. The value obtained with this model for the infrared-active mode A_{2u} was about 42 THz. Five years later this mode was found experimentally¹⁸ at 26.02 THz

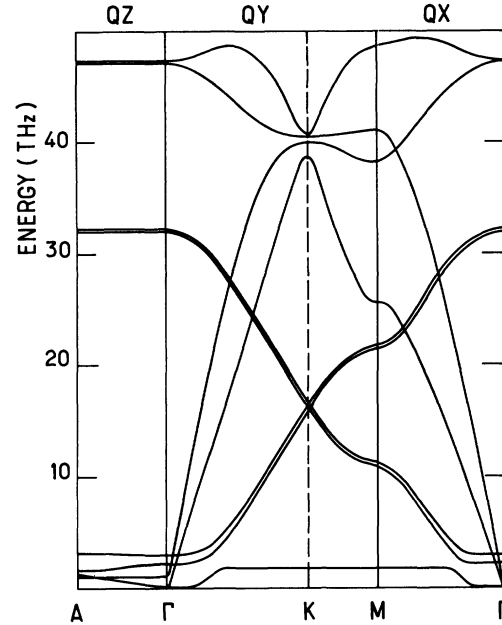


FIG. 8. Results of our phenomenological nonaxially symmetric Born–von Kármán calculation for the phonon dispersion relation of second-stage bromine GIC. The values of the parameters are summarized in Table III.

showing the inadequacy of the model.

To reduce this discrepancy Maeda *et al.*²¹ have made a new calculation of the phonon dispersion relation. They have used a Born–von Kármán force-constant model. They have taken into account the anisotropy of graphite by using anisotropic transverse force constants for the in-plane interactions. For each of these interactions they have introduced three force constants: ϕ_r radial, ϕ_{ii} transverse in the layer plane, and ϕ_{io} transverse perpendicular to the layers.

V. INTERPRETATION OF THE RESULTS

A. Main characters of the dispersion relation

An overall view of our results shows many similarities with those of pure HOPG which we have previously reported (Sec. IV). The range of the sound velocities and the range of the energies of acoustical branches are the same. In particular, the $[010]L$ branch has the same slope as in pure HOPG. This indicates that the corresponding coupling constants are probably the same.

However, both results present some clear differences: At low energy (<4 THz) there are three $[001]L$ branches instead of two in graphite. This is explained by the existence of a new identity period

TABLE I. Experimental frequencies (in THz) of the optical normal modes at $\vec{q}=0$ in graphite. The experimental techniques and the references are indicated.

Label	Mode			Experimental technique		
				Neutron scattering	Raman	Infrared
$E_{2g}^{(1)}$	→	→		1.44 ^a	1.26 ^d	
	←		←			
E_{1u}	→	←				47.61 ^c
	→		←			
$E_{2g}^{(2)}$	→	←			47.43 ^b	
	←		→			
$B_{1g}^{(1)}$	↑	↑		3.84 ^a		
	↓		↓			
A_{2u}	↑	↓				26.02 ^c
	↑		↓			
$B_{1g}^{(2)}$	↑	↓				
	↓		↑			

^aFrom Ref. 16.

^bFrom Ref. 17.

^cFrom Ref. 18.

^dFrom Ref. 19.

in this direction, which contains three layers instead of two. The presence of energy gaps is related to the existence of two kinds of layers: The carbon layers and the intercalated layers.

This feature was the basic of the rigid-layer model developed for another GIC.⁷ This also explains the existence of two optical [010]*T* branches which join the previous ones at the Γ point.

The observed [001]*TO* branch does not present any dispersion and we do not observe the acoustical one. In addition the energy of this flat branch seems to be $1/\sqrt{2}$ of that of the [001]*TO* branch of pure graphite at the Γ point. We can explain these features if we neglect the transverse coupling between the carbon and the intercalated layers. This also suggests that the transverse coupling between two adjacent carbon layers is probably the same as in pure graphite.

In spite of the fact that we have represented all our phonons in a unit cell different from the real one, we did not observe in the phonon spectrum any anomaly related to this choice. Two main reasons explain this fact. First, as the scattering lengths of a carbon atom (0.665×10^{-12} cm) and a bromine atom¹⁵ (0.68×10^{-12} cm) are very similar, the contribution to the scattering of the carbon atoms is about 14 times larger than that of bromine in our compounds ($C_{14}Br$). Secondly, as our sample is obtained

from HOPG only the isotropic branches around the *c* axis are easily observed. That is not the case for the phonons related to the intercalate layer which forms a rectangular cell. In conclusion, in order to explain these results a calculation which takes into account the cell in which we have indexed the phonons seems reasonable.

B. Calculation of the phonon dispersion relation

In order to explain our experimental results we have made a calculation of the phonon dispersion relation. We have elaborated a phenomenological Born–von Kármán model. In this model we have made some basic assumptions.

(1) We have neglected the electronic charge effects. In the acceptor GIC both the carbon and the intercalate layer are charged and through electron-phonon coupling this affects the phonon dispersion relation. This effect does not seem to be very important as is suggested by the energy shift of the high-frequency Raman-active mode² and may be masked by the choice of the phenomenological adjustable parameters of the model.

(2) In agreement with our results (Sec. V A) we have substituted the intercalate layer which has a well-defined order (Sec. II) by a continuous layer with the same weight density. Then we have calcu-

TABLE II. Analytical expressions of frequencies at the Γ point as calculated with our model. A schematic drawing showing the nature of the corresponding atomic vibrations is given in the left column.

→	→		0
→		→	
→	→		$\frac{1}{2\pi\sqrt{m}} \left\{ \frac{3}{2}(\phi_r^1 + \phi_{ii}^1) + \phi_i^{CC} - [(\phi_i^{CC})^2 + \frac{9}{4}(\phi_r^1 + \phi_{ii}^1)^2]^{1/2} \right\}^{1/2}$
←		←	
→	←		$\frac{1}{2\pi\sqrt{m}} [3(\phi_r^1 + \phi_{ii}^1)]^{1/2}$
→		←	
→	←		$\frac{1}{2\pi\sqrt{m}} \left\{ \frac{3}{2}(\phi_r^1 + \phi_{ii}^1) + \phi_i^{CC} + [(\phi_i^{CC})^2 + \frac{9}{4}(\phi_r^1 + \phi_{ii}^1)^2]^{1/2} \right\}^{1/2}$
←		→	
↑	↑		0
↑		↑	
↑	↑		$\frac{1}{2\pi\sqrt{m}} [\phi_r^{CI}(1+4\mu)]^{1/2}$
↑		↑	
		↓	
↑	↑		$\frac{1}{2\pi\sqrt{m}} \left\{ 3\phi_{io}^1 + \phi_r^{CC} + \phi_r^{CI} - [9(\phi_{io}^1)^2 + (\phi_r^{CC})^2]^{1/2} \right\}^{1/2}$
↓		↓	
↑	↓		$\frac{1}{2\pi\sqrt{m}} (6\phi_{io}^1 + \phi_r^{CI})^{1/2}$
↑		↓	
↑	↓		$\frac{1}{2\pi\sqrt{m}} \left\{ 3\phi_{io}^1 + \phi_r^{CC} + \phi_r^{CI} + [9(\phi_{io}^1)^2 + (\phi_r^{CC})^2]^{1/2} \right\}^{1/2}$
↓		↑	

lated the phonon-dispersion relation in the unit cell previously defined (Sec. V A) which contains three layers with four carbon atoms and one intercalate "pseudoatom."

We describe the interactions of the two carbon layers with an adaptation of the model of Maeda *et al.*²¹ for pure graphite (Sec. IV). Within the carbon layer we consider the interactions limited to the second-nearest neighbors with three parameters for each one: ϕ_r , ϕ_{ii} , and ϕ_{io} , radial, transverse in the layer plane, and transverse perpendicular to the layer, respectively. We have limited the interaction between adjacent carbon layers to the nearest neighbors and we describe it with two constants: ϕ_r^{CC} and ϕ_i^{CC} , radial and transverse, respectively. All these constants have been used in the calculation of Maeda *et al.* To describe the interaction between adjacent carbon and intercalate layers, which we have

also limited to the nearest neighbors, we have added two supplementary constants: ϕ_r^{CI} and ϕ_i^{CI} radial and transverse, respectively. We introduce the interaction between bromine pseudoatoms in order to take into account the real interaction between bromine atoms. We limit these interactions to the nearest neighbors and we describe them by three parameters: ϕ_r^{II} , ϕ_{ii}^{II} , and ϕ_{io}^{II} radial, transverse in the layer, and transverse perpendicular to the layer. m is the carbon atom mass and μ the ratio of the latter to that of the bromine "pseudoatom." Here $\mu=0.53$.

As we have five atoms in the unit cell the dynamical equation is a system of fifteen equations with thirteen adjustable parameters. As in graphite itself the modes polarized in the layers and perpendicular to the layers are uncoupled. For the modes polarized perpendicular to the layers we have a system of

five equations with five parameters: ϕ_r^{CC} , ϕ_r^{CI} , ϕ_{io}^1 , ϕ_{io}^2 , and ϕ_{io}^{II} and for the modes polarized in the layer plane we have a system of ten equations with eight parameters: ϕ_r^1 , ϕ_{ii}^1 , ϕ_r^2 , ϕ_{ii}^2 , ϕ_r^{II} , ϕ_{ii}^{II} , ϕ_r^{CC} , and ϕ_r^{CI} .

In agreement with our results we have made the additional assumption $\phi_r^{CI}=0$, which for the modes polarized in the layer plane uncouples the modes propagating in the carbon layers from the modes propagating in the intercalated layers. The first ones form a system of eight equations with five parameters ϕ_r^1 , ϕ_{ii}^1 , ϕ_r^2 , ϕ_{ii}^2 , and ϕ_r^{CC} and the second one a system of two equations with two parameters ϕ_r^{II} and ϕ_{ii}^{II} .

As we have made the approximation of the continuous layer for the intercalate layer the modes associated with this layer are not very realistic. We neglect them and we do not use the last two equations.

We have resolved this system of equations analytically for the Γ point and numerically for the higher-symmetry directions. In Table II we summarize the analytical expressions of the dispersion relations at the Γ point.

The modes polarized perpendicular to the layers form a system of five equations with five parameters that we adjust by using our experimental results on [001] L and [010] T phonon branches. With the three [001] L branches we adjust the ϕ_r^{CC} and ϕ_r^{CI} constants. But these branches depend also on ϕ_{io}^1 . The remaining three constants ϕ_{io}^1 , ϕ_{io}^2 , and ϕ_{io}^{II} are adjusted with the three [010] T branches. We adjust ϕ_{io}^1 and ϕ_{io}^2 with the two [010] TO branches. The [010] TA branch depends critically on ϕ_{io}^{II} but the [010] TO_1 only slightly.

The values of the parameters are summarized in Table III. In Fig. 3 we have superimposed on the experimental results the computed phonon dispersion relation at low energy in both the [001] direction and in the basal plane. The calculated [010] and [100] results are mixed in order to take into account the HOPG character of the sample.

The agreement between the experimental results and the calculated values is quite good for the [001] L branches except for the LO_2 branch where a systematic shift of about 3% is observed which is attributed to the charge effects. It is also good for the [001] TO branches but not for the acoustical one which depends mainly on ϕ_{io}^{II} . In Fig. 3 we take $\phi_{io}^{II}=0$ and we will discuss later (Sec. VI) this interaction between bromine pseudoatoms.

In order to adjust the force-constant parameters of the modes polarized in the layer plane we have used two independent experimental results: The high-frequency Raman-active mode $E_{2g}^{(2)}$ and the [001] T and [010] L phonon branches. As our previous discussion on these branches has suggested we

TABLE III. Numerical values of the force constants of our calculation in 10^2 N/m. The subscripts r indicate the radial component, ii the transverse in the layer plane, and io the transverse perpendicular to the layer plane.

Nearest neighbor in the layer	$\phi_r^1 = 3.066$ $\phi_{ii}^1 = 2.81$ $\phi_{io}^1 = 1.3561$
Second-nearest neighbor in the layer	$\phi_r^2 = 1.363$ $\phi_{ii}^2 = -0.527$ $\phi_{io}^2 = -0.220$
Nearest neighbor between adjacent carbon layer	$\phi_r^{CC} = 0.0579$ $\phi_r^{CC} = 0.00718$
Nearest neighbor between adjacent carbon and intercalate layer	$\phi_r^{CI} = 0.01228$ $\phi_r^{CI} = 0$
Nearest-neighbor interaction between bromine pseudoatom	$\phi_{io}^{II} = 0$

expect that the value of the corresponding parameters, ϕ_r^1 , ϕ_{ii}^1 , ϕ_r^2 , ϕ_{ii}^2 , and ϕ_r^{CC} , will be the same as in pure graphite.²¹ These values are summarized in Table III. The agreement with the experimental results is shown in Fig. 3 and is quite good for these branches. In Fig. 8 we show the complete results of the dispersion-relation computation for the high-symmetry directions with the parameters values given in Table III.

VI. DISCUSSION

Our model describes well the three [001] L branches at low energy (< 4 THz) and in particular the existence of energy gaps. We shall now compare this model to the rigid layers one previously used in order to explain the results in other GIC's.⁷ At the Γ point we find for the two lowest optical branches (Table II) the following expressions:

$$\nu_{O_1} = \left[\frac{\phi_r^{CI}(1+4\mu)}{m} \right]^{1/2},$$

$$\nu_{O_2} = \left[\frac{\phi_r^{CC} + \phi_r^{CI}}{m} \right]^{1/2} \left[1 - \frac{1}{12} \frac{\phi_r^{CC^2}}{\phi_{io}^1(\phi_r^{CC} + \phi_r^{CI})} \right],$$

with $\phi_r^{CC} \ll \phi_{io}^1$. The rigid-layer limit is given by $\phi_{io}^1 = \infty$. Then in this limit the ν_{O_2} energy is shifted up by about 0.3% but the ν_{O_1} value is not modified. In any case this shift is much smaller than the experimental one. We attribute the latter to the

charge-transfer effects which were also invoked to explain the shift of the high-energy Raman-active mode $E_{2g}^{(2)}$. The same shift was previously observed in donor GIC's and was tentatively explained with a shell phonon model.²²

In Table IV we summarize the calculated values at the Γ point. For the polarization along the c axis we find a high-energy infrared-active mode at 32.05 THz instead of 26.02 THz in pure graphite. This mode has not yet been observed. It will be interesting to find it in order to adjust the corresponding phenomenological constants more exactly.

If the agreement between the experimental results and the calculation is good for the [010]TO branches, this is not the case for the acoustical one. The reason of this disagreement is that the real interaction between bromine atoms in the actual layer is only simulated by introducing the interaction ϕ^{II} between bromine "pseudoatoms." The [010]TA branch depends critically on this interaction, the [010]TO₁ is affected mainly by hybridization when the acoustical one is very close whereas the [010]TO₂ branch is not affected by it.

Our calculation shows that the effects on the phonons related to the intercalate may be observed mainly in the [010]TA branch, but a more elaborated calculation of the [010]T branches must be done. We expect, for example, that the [010]TA branch gives after folding in the actual cell an acoustic and an optic branch with a gap in the zone boundary.

The shape of the [001]T branches is very particular: They are flat and the acoustic one could not be observed. In order to explain these facts we have taken $\phi_t^{CI}=0$. For this polarization the modes propagating in the carbon layers are uncoupled from those propagating in the intercalate layers. In particular the elastic constant $C_{44}=0$. This value must be considered as a limiting case which indicates that the real value is very small. Such a very small value of the C_{44} constant can be considered as characteristic of a layered material.

In the layer directions there would be two acoustic branches for each direction: One propagating in the carbon zones and another in the intercalate layers because both regions are uncoupled. However, a very small coupling between the two regions, which is necessary for the cohesion of the sample, is enough to change the upper "acoustic" branch which propagates in graphite into an optic one.

At the Γ point we have two high-energy optic-active modes: A Raman-active one and an infrared active. In Table IV we show the calculated values which are compared with the experimental ones. The difference between calculated and measured values is attributed to the charge effects² which are neglected in our calculation.

TABLE IV. The comparison between calculated and experimental values of the vibration modes at the Γ point for second-stage bromine GIC. These modes are referenced by schematic drawing of the corresponding atomic vibrations.

Mode	Calculated values	Experimental values		
		Neutron Scattering	Raman	Infrared
$\begin{array}{cc} \rightarrow & \rightarrow \\ \leftarrow & \leftarrow \end{array}$	0.95	0.95		
$\begin{array}{cc} \rightarrow & \leftarrow \\ \rightarrow & \leftarrow \end{array}$	47.31			47.60 ^(a)
$\begin{array}{cc} \rightarrow & \leftarrow \\ \leftarrow & \rightarrow \end{array}$	47.32		48.31	
$\begin{array}{ccc} \uparrow & \uparrow & \\ \uparrow & & \uparrow \\ & & \downarrow \end{array}$	2.20	2.20		
$\begin{array}{ccc} \uparrow & \uparrow & \\ \downarrow & & \downarrow \end{array}$	2.97	3.0		
$\begin{array}{ccc} \uparrow & \downarrow & \\ \uparrow & & \downarrow \end{array}$	32.09			
$\begin{array}{ccc} \uparrow & \downarrow & \\ \downarrow & & \uparrow \end{array}$	32.21			

^aThis result is given for FeCl₃ stage-2 GIC's (Ref. 2).

VII. CONCLUSION

We have studied by coherent inelastic neutron scattering the phonon-dispersion relation of second-stage bromine-graphite intercalation compound. The intercalate sample was obtained from HOPG. We have observed the almost complete low-energy (< 12 THz) dispersion relation with longitudinal and transverse phonons propagating along the c direction as well as in the layer plane.

The modes polarized along the c axis and in the basal plane are uncoupled. For the first ones we have observed three branches which present gaps in the c direction. The acoustic branch which is propagating in the basal plane is very sensitive to the intercalate in contrast to the optic ones. The main characteristic of the second ones is the dispersionless optic branch at about 1 THz in the c direction. In the basal plane the slope of the observed branch is similar to that of pure graphite. A phenomenological Born-von Kármán force-constant model with nonaxial symmetry developed in order to interpret our results explains them very well.

ACKNOWLEDGMENTS

We thank Mrs. M. Lelaurin for her help in the sample preparation, Dr. A. Moore who kindly fur-

nished us with HOPG samples, and Professor J. Bli-nowski who made his results available to us before publication.

-
- ¹*Intercalation Compounds of Graphite II, Synthetic Metals*, edited by F. Lincoln Vogel (Elsevier, Lausanne, 1981), Vols. 2 and 3.
- ²M. S. Dresselhaus and G. Dresselhaus, *Adv. Phys.* **30**, 139 (1981).
- ³J. J. Song, D. D. L. Chung, P. C. Eklund, and M. S. Dresselhaus, *Solid State Commun.* **20**, 1111 (1976); S. A. Solin, *Mater. Sci. Eng.* **31**, 153 (1977).
- ⁴C. Underhill, S. Y. Leung, G. Dresselhaus, and M. S. Dresselhaus, *Solid State Commun.* **29**, 769 (1979).
- ⁵W. D. Ellenson, D. Semmingsen, D. Guerard, D. G. Onn, and J. E. Fisher, *Mater. Sci. Eng.* **31**, 137 (1977).
- ⁶J. Rossat-Mignod, D. Fruchart, M. J. Moran, J. W. Milliken, and J. E. Fischer, *Synth. Met.* **2**, 143 (1980).
- ⁷A. Magerl and H. Zabel, *Phys. Rev. Lett.* **46**, 444 (1981).
- ⁸W. A. Kamitakahara, N. Wada, and S. A. Solin, *International Conference on Phonon Physics, Bloomington, Indiana, 1981* [*J. Phys. (Paris)* **C6**, 311 (1981)].
- ⁹C. Horie, M. Maeda, and Y. Kuramoto, *Physica B* **92**, 430 (1980).
- ¹⁰S. Y. Leung, G. Dresselhaus, and M. S. Dresselhaus, *Solid State Commun.* **38**, 175 (1981).
- ¹¹F. Batallan, I. Rosenman, C. Simon, G. Furdin, and H. Lauter, *International Conference on Phonon Physics, Bloomington, Indiana, 1981* [*J. Phys. (Paris)* **C6**, 344 (1981)].
- ¹²A. Herold, in *Physics and Chemistry of Materials with Layered Structures*, edited by F. Levy (Riedel, Dordrecht, 1979), Vol. 6, p. 323.
- ¹³W. T. Eeles and J. A. Turnbull, *Proc. R. Soc. London Ser. A* **283**, 179 (1965).
- ¹⁴I. Rosenman, F. Batallan, and G. Furdin, *Phys. Rev. B* **20**, 2373 (1979).
- ¹⁵B. Dorner and R. Comès, in *Dynamics of Solids and Liquids by Neutron Scattering*, edited by S. W. Lovesey and T. Springer (Springer, Berlin, 1977), p. 127.
- ¹⁶R. Nicklow, N. Wakabayashi, and H. G. Smith, *Phys. Rev. B* **5**, 4951 (1972).
- ¹⁷F. Tuinstra and J. F. Koenig, *J. Chem. Phys.* **53**, 1126 (1970).
- ¹⁸R. J. Nemanich, G. Lucovsky, and S. A. Solin, *Solid State Commun.* **23**, 117 (1977).
- ¹⁹R. J. Nemanich, G. Lucovsky, and S. A. Solin, in *Proceedings of the International Conference on Lattice Dynamics*, edited by M. Balkanski (Flammarion, Paris, 1975), p. 619.
- ²⁰G. Dolling and B. N. Brockhouse, *Phys. Rev.* **128**, 1120 (1969).
- ²¹M. Maeda, Y. Kuramoto, and C. Horie, *J. Phys. Soc. Jpn.* **47**, 337 (1979).
- ²²A. Magerl and H. Zabel, *International Conference on Phonon Physics, Bloomington, Indiana, 1981* [*J. Phys. (Paris)* **C6**, 329 (1981)].